Establishment and Characterization of a New Cell Line, A99, from a Primary Small Cell Carcinoma of the Pancreas

Shinichi Yachida, MD, PhD[1], **Yi Zhong, MD, PhD**[1], **Raul Patrascu, BS**[1], **Meghan B. Davis, MS**[1], **Laura A. Morsberger, BA**[1], **Constance A. Griffin, MD**[1,2], **Ralph H. Hruban, MD**[1,2], **Daniel Laheru, MD**[2], and **Christine A. Iacobuzio-Donahue, MD, PhD**[1,2,3]

[1]Department of Pathology, The Sol Goldman Pancreatic Cancer Research Center, Johns Hopkins Medical Institutions, Baltimore, MD

[2]Department of Oncology, The Sol Goldman Pancreatic Cancer Research Center, Johns Hopkins Medical Institutions, Baltimore, MD

[3]Department of Surgery, The Sol Goldman Pancreatic Cancer Research Center, Johns Hopkins Medical Institutions, Baltimore, MD

Abstract

Objectives—Small cell carcinoma (SCC) of the pancreas is a rare malignancy with a poor prognosis. We established and characterized a primary human pancreatic SCC cell line, designated A99.

Methods—Cancer tissue was obtained from the liver metastasis of a SCC of the pancreas and xenografted into nude mice. The first-pass xenograft was then used to establish a cultured cell line called A99. Cellular morphology, immunohistochemical properties, tumorigenic potential, and genetic alterations of this new line were characterized.

Results—A99 cells grew consistently in culture, formed colonies in soft agar and grew as subcutaneous xenografts when inoculated into nude mice. A99 cells were positive for pancytokeratin, synaptophysin, chromogranin A, NSE, CD57 (Leu7), CD56, PGP 9.5, TTF-1, Smad4, p53 and p16 but not for CD99, PDX-1 or RB protein. Sequencing analysis revealed homozygous point mutations of *KRAS* and *TP53*. Cytogenetic analysis revealed complex chromosomal rearrangements including marker chromosomes.

Conclusions—A99 is the first cell line report to be derived from a primary SCC of the pancreas. The establishment of this cell line may serve as a useful model system for studying the cell biology of this rare cancer, or for evaluation of novel targeted agents in preclinical models.

Keywords

cell line; small cell carcinoma; pancreas; neuroendocrine neoplasm; molecular genetics

Introduction

Primary small cell carcinoma (SCC) of the pancreas is an extremely rare malignancy. SCC of the pancreas is histologically defined by the presence of a diffuse, infiltrative growth

pattern, small to medium-sized cells with minimal cytoplasm, fusiform nuclei with finely granular chromatin pattern, and neuroendocrine differentiation. They are also notable for a high proliferative rate (more than 10 mitoses per 10 high-power fields or Ki-67 labeling index >20%) and abundant necrosis, similar to small cell carcinomas of the lung. The overall survival of patients with SCC of the pancreas varies between 2 and 5 months as most patients are diagnosed at an advanced stage of disease [12]. The origin of SCC of the pancreas is also a subject of debate. While some have proposed that the precursor to primary SCC of the pancreas may be an adenocarcinoma, others suggest that SCC is a variant of well-differentiated neuroendocrine neoplasms (islet cell tumors) or that epithelial stem cells might be the origin [3]. A standard treatment for unresectable SCC of the pancreas has not been established [4].

Immortalized cell lines are powerful tools for clarifying the biological characteristics of a cancer and for developing effective treatment strategies. A variety of cell lines derived from well-differentiated neuroendocrine neoplasms ("carcinoid tumors") have been established and characterized [56], however, no cell lines of primary SCC of the pancreas have been previously reported. We now report the establishment of a new cell line, A99, derived from a primary SCC of the pancreas and describe its characteristics with respect to sequencing, cytogenetic and immunohistochemical features.

Materials and Methods

Patient History

A 60-year-old Caucasian woman presented with a chief complaint of abdominal and back pain. There was no history of smoking or excess alcohol consumption. Her family history was unremarkable. She had no relevant previous medical or surgical history. On admission, physical examination revealed jaundice. Radiographic examination showed a mass, measuring 3.0 cm in diameter, within the head of the pancreas. The computed tomographic imaging of the chest and abdomen did not show any evidence of extra-pancreatic disease.

The patient underwent pylorus-preserving pancreaticoduodenectomy. Examination of the surgical specimen showed a 3.0 cm sized mass, invading the duodenal wall and common bile duct. On light microscopy, the neoplasm was composed entirely of small to medium-sized cells possessing scant cytoplasm and oval nuclei with a finely granular chromatin pattern (Figure 1a). The neoplasm showed extensive necrosis and a high frequency of mitotic figures (Figure 1a). Metastasis was identified in 10 of 23 sampled lymph nodes. Venous/lymphatic vessel and perineural invasion was also present. Complete review of all histologic sections did not reveal evidence of a component of ductal adenocarcinoma. Scattered pancreatic intraepithelial neoplasia-1 (PanIN-1) and 2 lesions were present in the background pancreas. The surgical resection margins were negative for neoplastic cells. The final pathological diagnosis was SCC of the pancreas with lymph node metastases.

Six weeks after surgical resection, the patient received chemotherapy consisting of cisplatin (60 mg/m^2) given intravenously on day 1 and etoposide (120 mg/m^2) intravenously on days 1–3, repeated every 3 weeks for three cycles. Three months after initial chemotherapy, a computed tomographic scan showed multiple liver metastases. The chemotherapy regimen was switched to obatoclax mesylate (GX15-070MS, 12.5 mg/m^2), a Bcl-2 antagonist, given intravenously on days 1 and 3 in combination with topotecan (1.25 mg/m^2) intravenously on days 1–5 but this second-line chemotherapy was ceased during the first cycle due to neutropenia. The patient's clinical course continued to deteriorate and she expired 13 months from the time of her surgery.

Prior to death, she consented to an autopsy for research purposes. At autopsy, multiple liver metastases, pleural studding of the lungs and peritoneum, and local recurrence were grossly identified. The local recurrence and multiple metastases were sampled and tumor tissues sliced into $1.0 \times 1.0 \times 0.2$ cm sections for overnight fixation in 10% buffered-formalin and for snap-freezing in liquid nitrogen. Histological examination confirmed the gross impression of recurrent SCC.

Autopsy Specimen Collection and Maintenance of Xenografts and Tumor Cell Line

One liver metastasis was obtained in sterile fashion, and 2 to 3 mm^3 samples were placed into sterile RPMI media (Invitrogen, Carlsbad, CA) for transport to the animal facility for xenografting into athymic nude mice that were maintained in a laminar-flow hood under pathogen-free conditions. Xenografting was performed as described by Hahn et al [7]. Tumor tissues were minced with a sterile blade into 1 mm^3 pieces in Matrigel (Becton Dickinson, Bedford, MA), and were implanted beneath the skin fold of the back bilaterally while the mice were under isoflourane inhalation anesthesia. The animals were followed weekly for growth of xenografts.

Cell Culture

When the xenografts reached ~10 mm in size, the tumors were excised and a portion of each was placed in 10% formalin for paraffin embedding or snap frozen in preparation for subsequent genetic analyses. A final portion was placed in DMEM medium with 20% fetal bovine serum (FBS), minced with sterile blades and digested with collagenase, type IV (Invitrogen), and hyaluronidase (Sigma-Aldrich, St. Louis, MO) for 30 minutes. The digested cells were centrifuged 10 minutes at 1,000 rpm and resuspended into DMEM culture media supplemented with 20% FBS, penicillin 100 U/mL, streptomycin 100 μg/mL, gentamicin 50 μg/mL and amphotericin B 2.5 μg/mL at 37°C in a humidified atmosphere containing 5% CO_2 and 95% air. The supernatant with solid remnants was removed 24 hours later and replaced with fresh medium. Cells were passaged at 50% to 100% confluence and medium was exchanged every 2 days. Cell cultures were routinely monitored for mycoplasma contamination, and no mycoplasma growth has been detected.

Colony Formation in Soft Agar

Six-well plates were filled with semisolid medium containing DMEM, 1% Bacto agar and 20% FBS and 50,000 cells in a semisolid medium (DMEM with 1% Bacto agar and 10% FBS) were added per well. Additional medium (DMEM with 20% FBS, penicillin, streptomycin, gentamicin and amphotericin B) was added to the wells to keep the agar moist, and 2.5 mL of fresh medium were added to each well every 3 days thereafter. After incubation for 21 days at 37°C, to assess colony formation, the medium was removed, and 3 mL of 0.005% Crystal Violet (Sigma-Aldrich) staining solution was added to each well. After incubation at 37°C for 3 hours, removal of the staining solution and washing twice with phosphate-buffered saline (PBS), colonies were visualized by trans-UV illumination and counted using the analysis software Quantity One (Bio-Rad, Hercules, CA).

Tumorigenicity in Nude Mice

A99 cells at passage 15 were grown to 80% confluence and trypsinized, and >90% cell viability was confirmed by trypan blue exclusion. Three 5-weeks-age athymic nude mice were subcutaneously(s.c.) inoculated into the back bilaterally. 0.5×10^7 or 1.7×10^7 of A99 cells of two different passages in 200 μL of PBS were used for each injection. The mice were observed weekly for the development of xenografts. At 8 weeks after injection, the s.c. xenografted tumors reached a diameter of 13–22 mm. The mice were sacrificed and the s.c.

tumors formed from A99 cells were excised and a portion of each was placed in 10% formalin for paraffin embedding or snap frozen in liquid nitrogen.

Immunohistochemistry

The tissue samples of the patient's original tumor specimen, first passage xenografts and the s.c. tumor formed from A99 cells were formalin-fixed and paraffin-embedded. Paraffin blocks were cut into sections 4 μm thick for the immunolabeling by the avidin-biotin complex method, with all labeling processes, from deparaffinization to counterstaining with hematoxylin, being performed automatically with the Ventana Discovery staining system (Ventana Medical Systems, Tucson, AZ). Antibodies used for immunohistochemical labeling are summarized in Table 1.

DNA Extraction and Sequencing for *KRAS, p16* and *TP53*

Genomic DNA was extracted from A99, its corresponding xenograft and the original metastatic tissue from which it was derived at autopsy using standard phenol-chlorophorm-isoamyl alcohol method or DNeasy Blood & Tissue Kits (Qiagen, Valencia, CA). Polymerase chain reactions (PCR) of *KRAS* exons 1 and 2, *p16* exons 1 and 2 and *TP53* exons 5 to 9 were performed as described [8]. PCR products were sequenced by use of a universal M13F primer that was incorporated into the forward primer of each primer pair (Beckman Coulter Genomics, Danvers, MA). Sequence data were analyzed with Sequencher 4.10.1 software (Gene Codes, Ann Arbor, MI).

Chromosome Analysis

The cell culture was harvested with exposure to 10 ng/mL Colcemid for 4 hours, incubated in cancer hypotonic solution at 37°C for 30 minutes, and fixed in 3:1 methanol:glacial acetic acid. Trypsin-Leishman staining procedure was used for G-band karyotyping. Chromosomal abnormalities were described using ISCN 2009 nomenclature [9].

Results

Cell Morphology of the Cell Line

Neoplastic tissue was obtained from the liver metastasis of the SCC of the pancreas and xenografted into nude mice. This xenograft was used to create cell line A99. A99 grew constantly and formed tubular clusters but occasionally grape-like cell aggregates noted under phase contrast microscopy (Figure 2). The cultured cells were composed of small cells with granular cytoplasm and round-oval nuclei with finely stippled chromatin. A99 cells maintained their growth when cultured on poly-L-lysine-coated plastic flasks but not on uncoated plastic tissue culture flasks. Typically, aggregates of the small cells loosely adhered to the poly-L-lysine-coated plastic flasks and some cells detached before reaching confluence. Overall, these features were maintained in this cell line at 80 passages and are now considered stable.

Colony Formation in Soft Agar

A99 cells were plated in soft agar at 50,000 per well in three wells in a six-well plate. They formed 173, 157 and 139 colonies per well on a six-well plate at 21 days after having been plated in soft agar (Figure 3).

Tumorigenicity *In Vivo*

Subcutaneous injections of up to 1.7×10^7 viable cells of two different passages into three nude mice have resulted in tumor development in all mice. After 8 weeks, tumors reached a diameter of 13–22 mm and grew as discrete encapsulated masses, without evidence of local

invasion or distant metastasis. Tumors were harvested and assessed histologically. In all cases, the harvested xenografts were identical histologically to the patient's original resected SCC (Figure 1). Necrosis was abundant and mitotic figures were highly frequent.

Immunohistochemistry

Table 2 summarizes the immunohistochemical findings for this tumor. The neoplastic cells labeled with antibodies to pancytokeratin (AE1/AE3), synaptophysin, chromogranin A (Figure 4a), NSE, CD57 (Leu7), CD56, PGP 9.5, thyroid transcription factor-1 (TTF-1), Smad4, p53 and p16, but not with antibodies to CD99, PDX-1 and retinoblastoma (RB) protein (Figure 4b). The Ki-67 labeling index was 59.7% (2124/3556). The immunohistochemical labeling patterns of all proteins were identical in the patient's original carcinoma, first passage xenografts, A99 cells or the s.c. tumor formed from A99 cells.

Sequencing Analysis of *KRAS, p16* and *TP53* Genes

Homozygous dinucleotide point mutations of *KRAS* were identified at codon 12 (Glycine to Leucine, GGT to CTT). A homozygous *TP53* mutation was present at codon 127 (Serine to Threonine, TCC to ACC). No *p16* mutations were found. There were no differences in these mutational signatures of samples between frozen tissues from patient's original tumor, first passage xenografts and the cultured cell line (Figure 5).

Chromosome Studies

Chromosomal analysis of A99 cells in G-banding showed the following clonal abnormalities in the 20/20 well-spread metaphases examined (Figure 6): 57~68<3n>, X,-X,der(X;2)(q10;p10),t(2;5)(q21;q13),der(5)t(2;5)del(5)(q11.2q13),+7,i(8)(q10)x2, der(9)t(1;9)(q25;p13)ins(9;?)(p13;?)dup(?),−10,i(10)(q10), −12,−14,−15,−17,der(17)t(8;17)(q12;p11.2),−19,−22,+3~5mar[20].

Discussion

While 96% of SCCs are of pulmonary origin, about 4% arise in extrapulmonary sites. The most common sites of origin are the gastrointestinal system, larynx, pharynx and paranasal sinuses, uterus, cervix and prostate [10][11][12]. SCC arising in the pancreas is an extremely rare entity. A Medline search of the literature indicated only 40 cases were reported from 1973 through 2009. Consistent with our patient, SCC of the pancreas is likely to occur in the head of pancreas in patients with average age of 60 years and common clinical manifestations are abdominal pain, weight loss and jaundice [2]. The identification, development, and testing of therapeutic agents for SCC of the pancreas have been hampered by the lack of available models. For these reasons, the establishment of a cell line of SCC of the pancreas that could help to understand the histogenesis and lead to appropriate treatment has been eagerly anticipated. A human pancreatic carcinoid cell line, BON, has been widely used to study pancreatic neuroendocrine tumors, but carcinoid tumors are both clinically and genotypically distinct from SCC of the pancreas [5]. The A99 cell line grows continuously in cell culture, forms colonies in soft agar, forms solid tumors when injected s.c. into nude mice, and expresses numerous neuroendocrine markers. This line also retains the characteristics of the patient's original carcinoma by morphologic examination, immunohistochemical studies and sequencing analysis. The ability of this cell line to reliably form tumors *in vivo* may thus enable preclinical studies to test antineoplastic agents on SCCs of the pancreas.

Molecular analyses of A99 indicate it is genetically complex. In karyotype analysis, both numerical and structural chromosome abnormalities were identified. These changes are similar to the patterns of chromosomal aberrations reported for high-grade neuroendocrine

carcinomas including small cell cancers of the lung, which have recurrent numerical whole-chromosome losses, frequently involving chromosomes 4, 10, 15 and 22 and structural aberrations including deletions of chromosomes 1p, 3p, 5q, 10q, and 17p [13]. Sanger sequencing of the carcinoma and cell line revealed an activating mutation of *KRAS* and an inactivating mutation of *TP53*. The *KRAS* mutation found is a rare dinucleotide ("tandem") mutation in codon 12 that is nonetheless predicted to have oncogenic function [14]. Of interest, while p16 expression was intact there was a complete loss of RB protein by immunohistochemistry. Loss of RB protein is rare in both pancreatic ductal adenocarcinoma and neuroendocrine neoplasms [15,16] whereas it is frequently observed in small cell carcinomas of the lung and in SCCs in extrapulmonary sites [17,18]. In human and mouse models of small cell lung carcinoma, loss of p53 and RB activities are a necessary step of the genetic progression and aberrations of *RB1* gene play an important role in the carcinogenesis in terms of neuroendocrine features [19,20,21].

In conclusion, we have developed a SCC cell line capable of being propagated in tissue culture and in nude mice. Prospective randomized trials of therapy for SCC of the pancreas are unlikely in the future because of the rarity of the disease. This cell line, A99, has promise as a valuable tool for investigating the biology of SCC and for developing preclinical therapeutic models to treat this aggressive tumor type.

Acknowledgments

References

1. Nakamura Y, Tajiri T, Uchida E, et al. Changes to levels of serum neuron-specific enolase in a patient with small cell carcinoma of the pancreas. J Hepatobiliary Pancreat Surg. 2005; 12:93–8. [PubMed: 15754108]

2. Chung MS, Ha TK, Lee KG, et al. A case of long survival in poorly differentiated small cell carcinoma of the pancreas. World J Gastroenterol. 2008; 14:4964–7. [PubMed: 18756608]

3. Wang RF, Chou YH, Hwang JI, et al. Primary small cell carcinoma of the pancreas with an unusual sonographic appearance. J Clin Ultrasound. 2007; 35:82–4. [PubMed: 17206725]

4. Iwasa S, Morizane C, Okusaka T, et al. Cisplatin and etoposide as first-line chemotherapy for poorly differentiated neuroendocrine carcinoma of the hepatobiliary tract and pancreas. Jpn J Clin Oncol. 2010; 40:313–8. [PubMed: 20047862]

5. Evers BM, Ishizuka J, Townsend CM Jr, et al. The human carcinoid cell line, BON. A model system for the study of carcinoid tumors. Ann N Y Acad Sci. 1994; 733:393–406. [PubMed: 7978888]

6. Tillotson LG, Lodestro C, Hocker M, et al. Isolation, maintenance, and characterization of human pancreatic islet tumor cells expressing vasoactive intestinal peptide. Pancreas. 2001; 22:91–8. [PubMed: 11138979]

7. Hahn SA, Seymour AB, Hoque AT, et al. Allelotype of pancreatic adenocarcinoma using xenograft enrichment. Cancer Res. 1995; 55:4670–5. [PubMed: 7553647]

8. Embuscado EE, Laheru D, Ricci F, et al. Immortalizing the complexity of cancer metastasis: genetic features of lethal metastatic pancreatic cancer obtained from rapid autopsy. Cancer Biol Ther. 2005; 4:548–54. [PubMed: 15846069]

9. Shaffer, LGS.; ML; Campbell, LJ. An International System for Human Cytogenetic Nomenclature. Basel: S Karger; 2009.

10. Yachida S, Matsushita K, Usuki H, et al. Long-term survival after resection for small cell carcinoma of the esophagus. Ann Thorac Surg. 2001; 72:596–7. [PubMed: 11515903]

11. Brennan SM, Gregory DL, Stillie A, et al. Should extrapulmonary small cell cancer be managed like small cell lung cancer? Cancer. 2010; 116:888–95. [PubMed: 20052730]

12. Wang W, Epstein JI. Small cell carcinoma of the prostate. A morphologic and immunohistochemical study of 95 cases. Am J Surg Pathol. 2008; 32:65–71. [PubMed: 18162772]

13. Welborn J, Jenks H, Taplett J, et al. High-grade neuroendocrine carcinomas display unique cytogenetic aberrations. Cancer Genet Cytogenet. 2004; 155:33–41. [PubMed: 15527900]

14. Feldser DM, Kern SE. Oncogenic levels of mitogen-activated protein kinase (MAPK) signaling of the dinucleotide KRAS2 mutations G12F and GG12-13VC. Hum Mutat. 2001; 18:357. [PubMed: 11668624]

15. Gerdes B, Ramaswamy A, Ziegler A, et al. p16INK4a is a prognostic marker in resected ductal pancreatic cancer: an analysis of p16INK4a, p53, MDM2, an Rb. Ann Surg. 2002; 235:51–9. [PubMed: 11753042]

16. Delle Fave G, Corleto VD. Oncogenes, growth factors, receptor expression and proliferation markers in digestive neuroendocrine tumours. A critical reappraisal. Ann Oncol. 2001; 12 (Suppl 2):S13–7. [PubMed: 11762339]

17. Takubo K, Nakamura K, Sawabe M, et al. Primary undifferentiated small cell carcinoma of the esophagus. Hum Pathol. 1999; 30:216–21. [PubMed: 10029452]

18. Parwani AV, Geradts J, Caspers E, et al. Immunohistochemical and genetic analysis of non-small cell and small cell gallbladder carcinoma and their precursor lesions. Mod Pathol. 2003; 16:299–308. [PubMed: 12692194]

19. Cagle PT, el-Naggar AK, Xu HJ, et al. Differential retinoblastoma protein expression in neuroendocrine tumors of the lung. Potential diagnostic implications. Am J Pathol. 1997; 150:393–400. [PubMed: 9033254]

20. Kaye FJ, Harbour JW. For whom the bell tolls: susceptibility to common adult cancers in retinoblastoma survivors. J Natl Cancer Inst. 2004; 96:342–3. [PubMed: 14996847]

21. Meuwissen R, Linn SC, Linnoila RI, et al. Induction of small cell lung cancer by somatic inactivation of both Trp53 and Rb1 in a conditional mouse model. Cancer Cell. 2003; 4:181–9. [PubMed: 14522252]
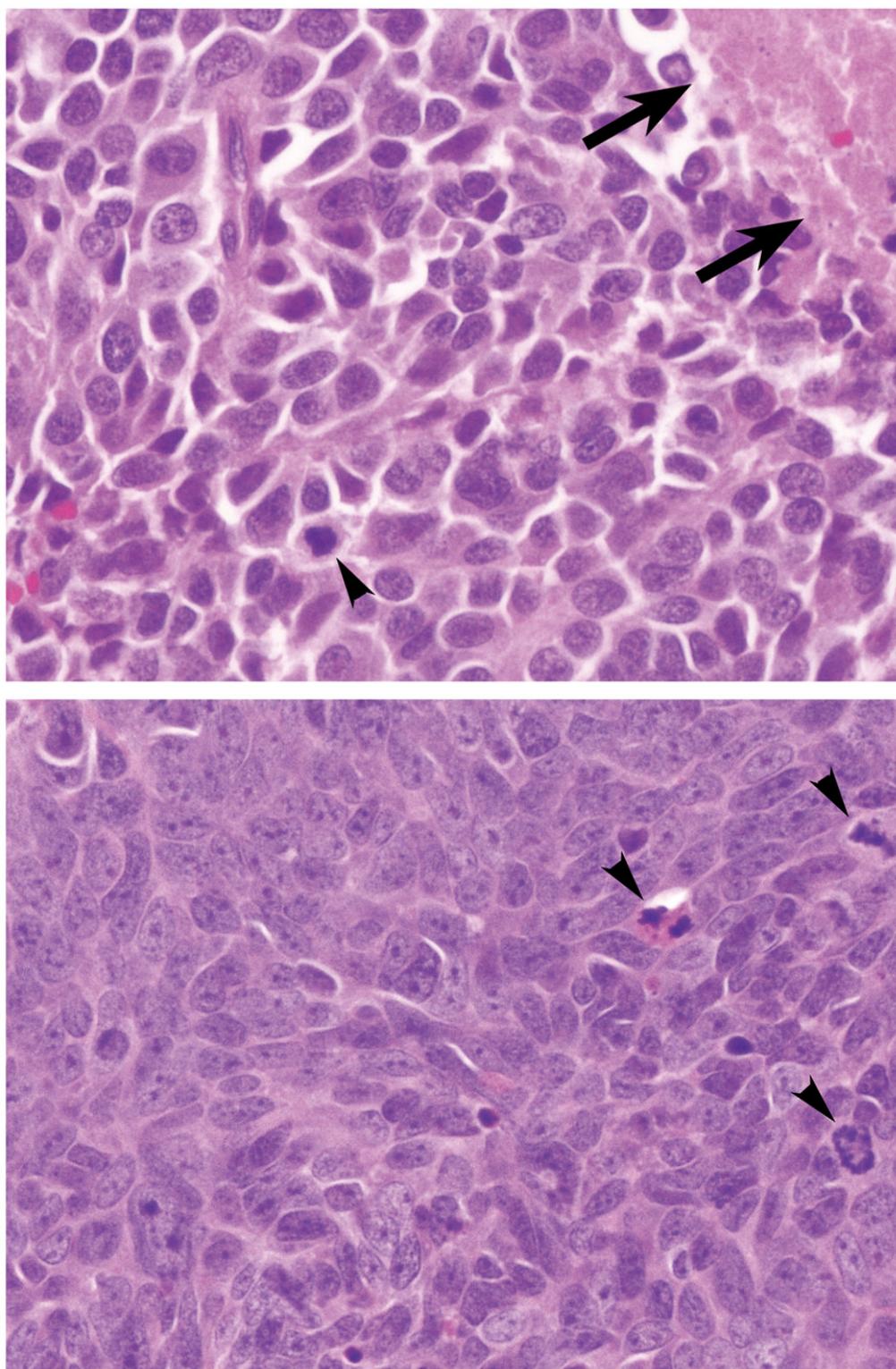
Figure 1.
Photomicrographs of primary small cell carcinoma of the pancreas (patient's original tumor)
(**a**) and heterotransplanted tumor tissue in a nude mouse inoculated with A99 (**b**)

demonstrating similar histopathologic characteristics. Necrosis (*arrows*) and mitotic cells (*arrowheads*) are present. Hematoxylin and eosin stain (original magnification **a** and **b** x400).
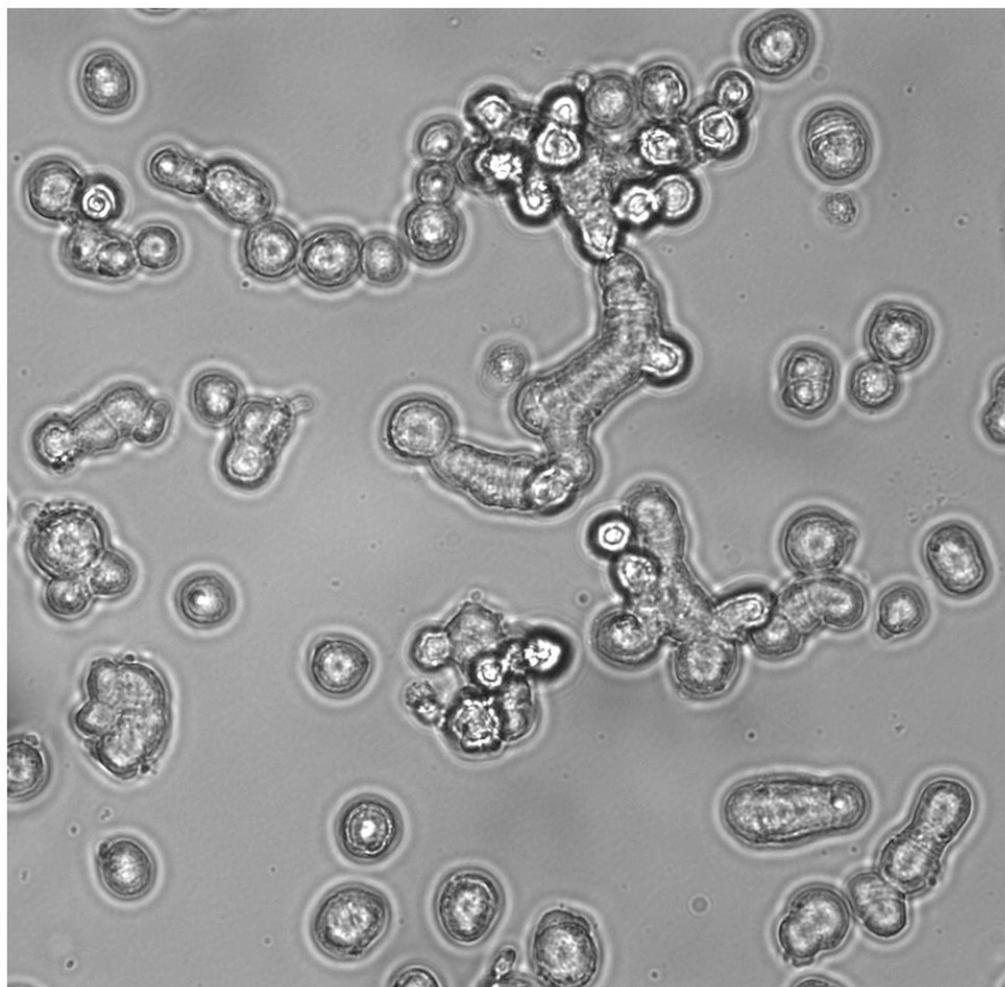
Figure 2.
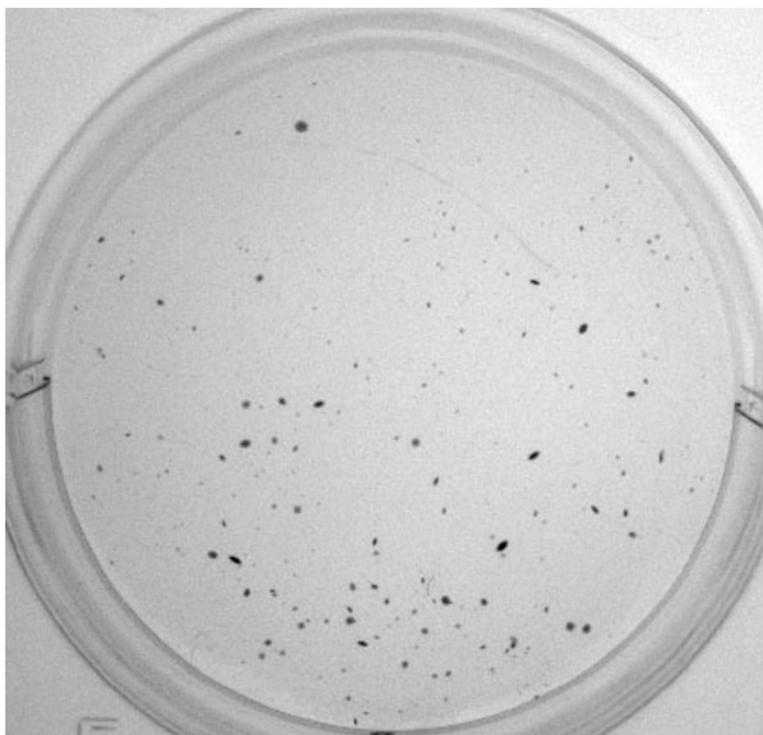Inverted phase contrast microscope examination of A99 cells (original magnification x200).

Figure 3.
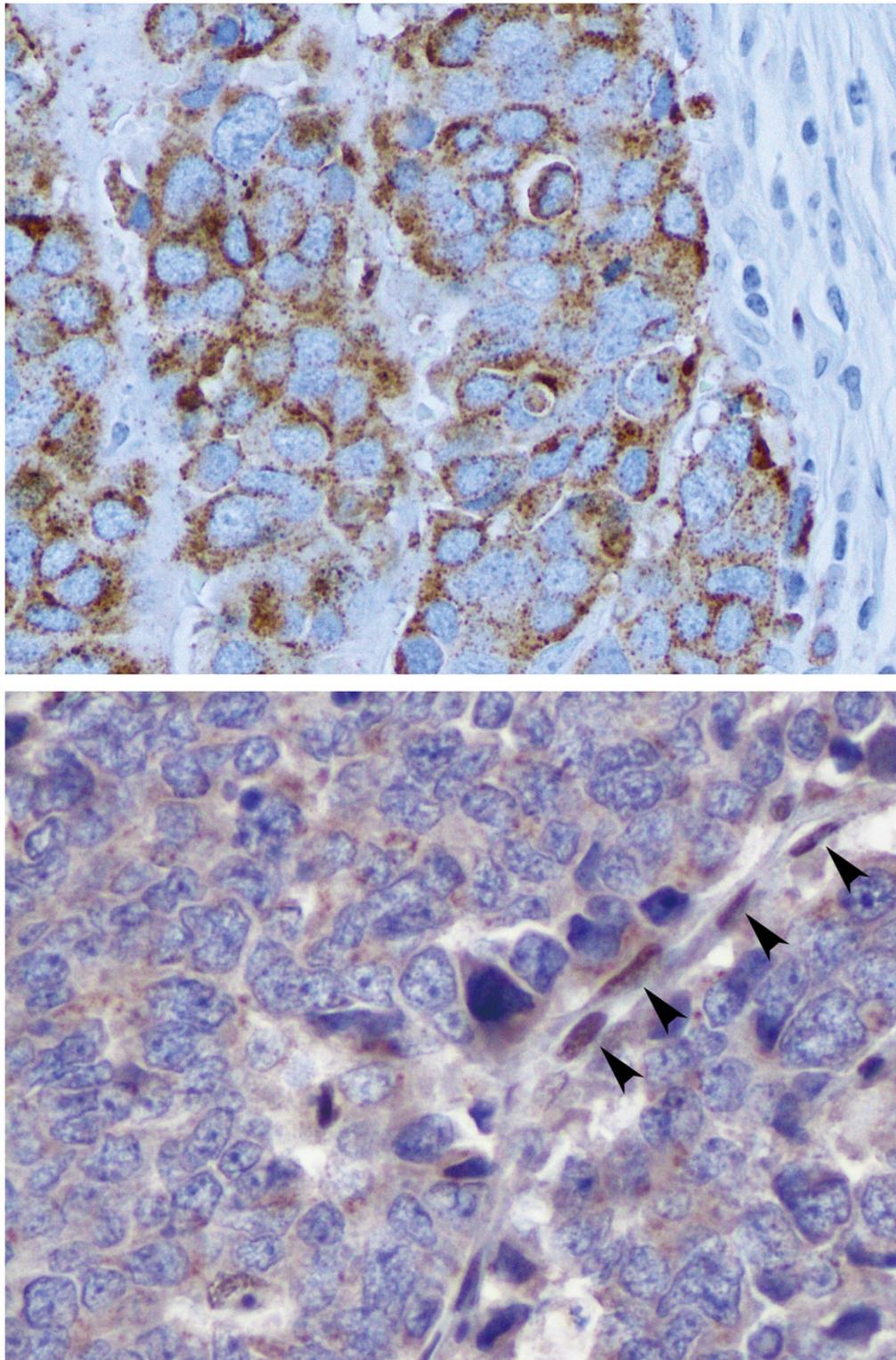Colony formation assay in soft agar.

Figure 4.
Immunohistochemical labeling of the patient's original tumor. (**a**) The tumor cells were diffusely positive for chromogranin A (original magnification, x400). (**b**) The tumor cells

showed negative nuclear labeling for retinoblastoma (RB) protein. Active fibroblasts within the tumor were regarded as internal positive controls for this protein (***arrowheads***) (original magnification, x400).
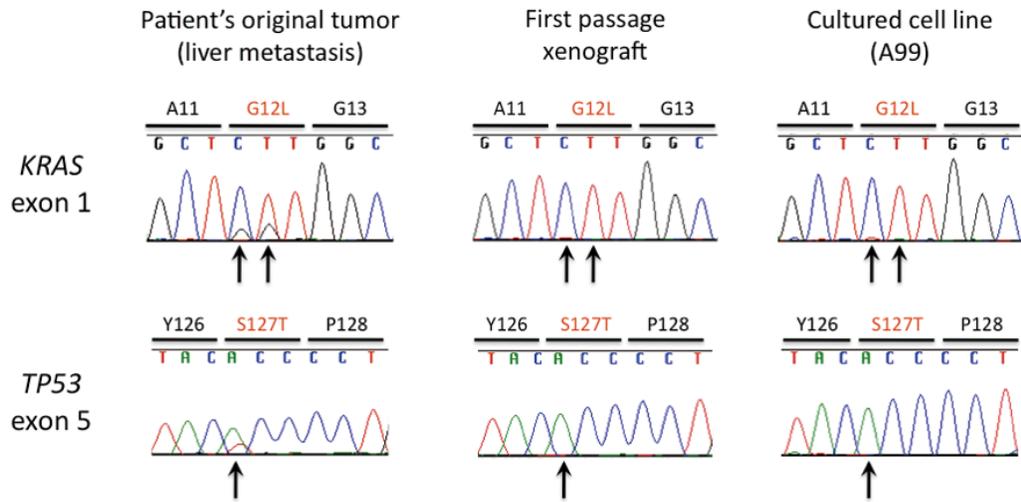
Figure 5.
Sequencing analysis for *KRAS* and *TP53* in the patient's original tumor, the first passage xenograft and the cultured A99 cell line. Dinucleotide *KRAS* mutations and a *TP53* mutation are present (indicated by ***arrows***).
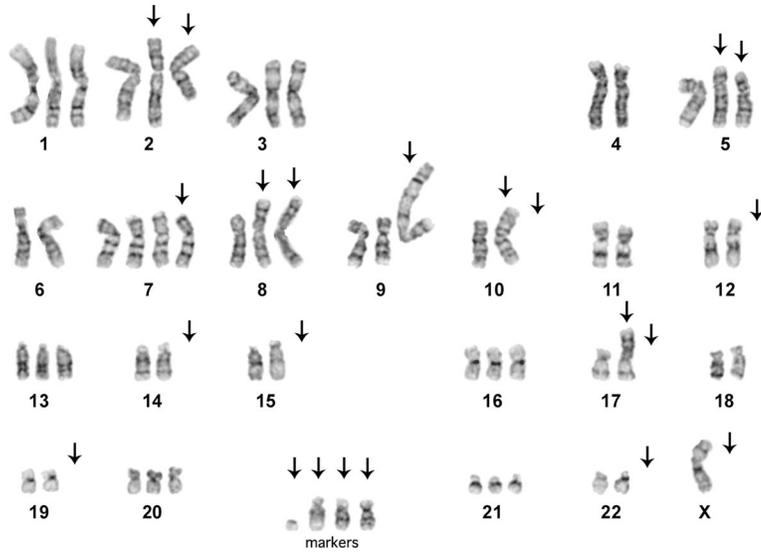
Figure 6.
Cytogenetic analysis of *in vitro* passage 25 in A99 cells. There are many complicated chromosomal rearrangements including marker chromosomes.

Table 1

Antibodies used in the immunohistochemical study

Antibody (clone)	Source	Dilution	Incubation time
Cytokeratin (Pan) (AE1/AE3&PCK26)	Ventana, Tucson, AZ	Ready-to-use	RT, 16 minutes
Synaptophysin (27G12)	Novacastra, Wetzlar, Germany	1:4000	RT, 35 minutes
Chromogranin A (LK2H10)	Ventana	Ready-to-use	RT, 16 minutes
NSE (E27)	Ventana	Ready-to-use	RT, 32 minutes
CD57 (Leu7) (NK-1)	Ventana	Ready-to-use	RT, 32 minutes
CD56 (123C3)	Ventana	Ready-to-use	RT, 32 minutes
PGP 9.5	DakoCytomation, Grustrup, Denmark	1:500	RT, 2 hours
TTF-1 (8G7G3/1)	Ventana	Ready-to-use	RT, 32 minutes
CD99 (O13)	Ventana	Ready-to-use	RT, 32 minutes
Smad4 (B-8)	Santa Cruz Biotechnology, Santa Cruz, CA	1:100	RT, 3 hours
p53 (Bp-53-11)	Ventana	Ready-to-use	RT, 16 minutes
Retinoblastoma protein (3C8)	QED Bioscience, SanDiego, CA	1:1000	RT, 1 hour
p16 (E6H4)	mtm laboratories, Heidelberg, Germany	Ready-to-use	RT, 28 minutes
PDX-1 (clone 267712)	R&D Systems, Minneapolis, MN	1:50	RT, 15 minutes
Ki-67 (30–9)	Ventana	Ready-to-use	RT, 16 minutes

RT, room temperature; NSE, neuron specific enolase; PGP 9.5, protein gene product 9.5; TTF-1, thyroid transcription factor-1.

Table 2

Immunohistochemistry of primary patient's original tumor, xenografted tumor and s.c. tumor formed from A99 cells

Antibody	Normal islet cells	Original patient's tumor	First passage xenograft	s.c. tumor formed from A99 cells
Cytokeratin (Pan)	+ (focally)	+	+	+
Synaptophysin	+	+ (focally)	+ (focally)	+ (focally)
Chromogranin A	+	+	+	+ (focally)
NSE	+	+ (focally)	+	+
CD57 (Leu7)	+ (focally)	+ (focally)	+	+
CD56	+	+	+	+
PGP 9.5	+	+	+	+
TTF-1	−	+	+	+ (focally)
CD99	−	−	−	−
Smad4	+ (focally)	+	+	+
p53	−	+	+	+
Retinoblastoma protein	+	−	−	−
p16	+ (focally)	+	+	+
PDX-1	+	−	N/A	N/A

NSE, neuron specific enolase; PGP 9.5, protein gene product 9.5; TTF-1, thyroid transcription factor-1.